Biochimica et Biophysica Acta 1818 (2012) 103–116

Contents lists available at SciVerse ScienceDirect

Biochimica et Biophysica Acta

journal homepage: www.elsevier.com/locate/bbamem

Effect of surfactant concentration, compression ratio and compression rate on the surface activity and dynamic properties of a lung surfactant

Sameh M.I. Saad [a], Zdenka Policova [a], Edgar J. Acosta [a,b], A. Wilhelm Neumann [a,*]

[a] Department of Mechanical and Industrial Engineering, University of Toronto, 5 King's College Road, Toronto, Ontario, Canada M5S 3G8
[b] Department of Chemical Engineering and Applied Chemistry, University of Toronto, 200 College Street, Toronto, Ontario, Canada M5S 3E5

ARTICLE INFO

Article history:
Received 15 March 2011
Received in revised form 17 September 2011
Accepted 3 October 2011
Available online 12 October 2011

Keywords:
Pulmonary surfactant
Compression Relaxation Model
ADSA–CSD
Relaxation
Adsorption
Elasticity

ABSTRACT

This paper reports dynamic surface tension experiments of a lung surfactant preparation, BLES, for a wide range of concentrations, compression ratios and compression rates. These experiments were performed using Axisymmetric Drop Shape Analysis–Constrained Sessile Drop (ADSA–CSD). The main purpose of the paper is to interpret the results in terms of physical parameters using the recently developed Compression–Relaxation Model (CRM). In the past, only the minimum surface tension was used generally for the characterization of lung surfactant films; however, this minimum value is not a physical parameter and depends on the compression protocol. CRM is based on the assumption that the dynamic surface tension response is governed by surface elasticities, adsorption and desorption of components of the lung surfactant. The ability of CRM to fit the surface tension response closely for a wide variety of parameters (compression ratio, compression rate and surfactant concentration) and produce sensible values for the elastic and kinetic parameters supports the validity of CRM.

1. Introduction

Pulmonary surfactants are mixtures of lipids and proteins suspended as vesicles or other aggregates in the alveolar fluid. These lipids and proteins can spread to form a monolayer or possibly multilayers at the alveolar liquid–air interface. The key property of lung surfactants is their dynamic surface tension response to film compression and expansion. The surfactant at the interface modulates the surface tension of the lung, lowering the normal air–water surface tension of approximately 70 mJ/m^2 to extremely low values below 5 mJ/m^2 [1].

Respiratory distress syndrome (RDS) is a clinical condition defined by the onset of poor blood oxygenation due to lung injury, and lack or malfunction of lung surfactant [1]. RDS is typically classified into neonatal RDS (nRDS) and acute RDS (ARDS) [1,2]. Exogenous surfactant replacement therapy, in which either synthetic or modified natural pulmonary surfactant (extracted from bovine or porcine sources) is delivered into the patients' lungs, has been established as a standard therapeutic intervention for patients with nRDS [3]. Surfactant therapy has shown limited therapeutic effect on ARDS patients [4–7].

In these therapies, high concentrations of the exogenous surfactant are commonly used to reach an effective dose, i.e. the surfactant dose to recover the mechanical properties of the lungs. The dose is usually in the range of 8 mg/ml [1,8,9]. Some other formulations, e.g. bovine lipid extracted surfactant (BLES) preparations, are used in surfactant replacement therapy with larger doses of 27 mg/ml [10].

On the other hand, there is still a lack of in vitro studies for these high concentrations, partly due to limitations of methodologies used. For these studies, the maximum surfactant concentration is usually restricted to no more than 3 mg/ml. This restriction arises from optical limitations since surfactant suspensions become murky and eventually opaque at increased concentrations.

Although there is promising evidence for surfactant therapy in ARDS, the effectiveness of high doses of commercial surfactant preparations has been inconsistent in clinical trials [11–13,7,14,15]. However, surfactant concentration is only one strategy to address the problem. High frequency low tidal volume ventilation, henceforth simply referred to as high frequency ventilation (HFV) has been shown to reduce, even if marginally, the mortality of ARDS [12,16–20].

Desirable features of surface tension methodologies include accurate measurements at near zero surface tensions (requiring absence of film leakage) under dynamic conditions. It is necessary to pre-humidify the air at body temperature, to be consistent with physiological conditions [10,21,22]. To simulate normal breathing, cycling frequencies of 0.1–0.5 Hz and a reduction in surface area near 20% are necessary [23,2,1]. However, for high frequency ventilation it is necessary to produce cycling frequencies higher than 1 Hz [24]. Furthermore, it is important to note that turbid concentrated suspensions are used in clinical practice [1,8]. To evaluate the effect of gases, aerosols, inhibitors, surfactant additives, and to deposit mixed lipid films it is useful to gain access to the air-water interface from the air and from the aqueous phase. The constrained sessile drop (CSD) configuration in conjunction with Axisymmetric Drop

* Corresponding author. Tel.: +1 416 978 1270; fax: +1 416 978 7753.
E-mail address: neumann@mie.utoronto.ca (A.W. Neumann).

0005-2736/$ – see front matter © 2011 Elsevier B.V. All rights reserved.
doi:10.1016/j.bbamem.2011.10.004

Shape Analysis (ADSA), illustrated in Fig. 1, features all these capabilities [25–27]. Other methodologies do not necessarily allow the straightforward changes in experimental parameters. For example, Langmuir–Wilhelmy balances do not allow for compression at high frequencies because of the formations of waves on the surface [23,28–30].

The captive bubble (CB) is noteworthy in that it avoids all possible pathways for film leakage, but it has been shown that it is not suitable for concentrated turbid suspensions (concentrations higher than 3 mg/ml) [2,31,32,33]. However, recent experiments use sub-phase spreading of highly concentrated suspensions near the interface [Schurch, 2010].

In the ADSA–CSD setup, a sessile drop is formed on top of a small flat pedestal with a circular sharp knife edge preventing uncontrolled spreading and hence film leakage [25–27]. ADSA–CSD is used to perform dynamic cycling by successive compression/expansion of the drop via programmed cycling of the drop volume. This is normally done through several cycles (normally 20) with prescribed periodicity and compression ratio (percentage of surface area reduction). In such experiments, a large amount of data is collected including the surface tension as a function of time as well as the change of the drop surface area and volume. Such results can provide valuable information about various properties of the film.

To assess the performance of surfactant preparations subject to dynamic compression/expansion, typically only the minimum surface tension at the end of compression is reported. While the minimum surface tension is useful for a preliminary assessment, it has to be realized that it is not a thermodynamic or other physical property as it depends on the method of compression [34]. Increasing the extent of compression or the speed of compression may significantly change the value of the minimum surface tension observed [10]. In fact, this makes the comparison of different literature values difficult in the case of different compression protocols. Therefore, it is necessary to concentrate on the properties of the film itself such as its elasticity, its formation (adsorption) and its stability (or relaxation tendency) as proposed in the literature [10,35] in addition, if not in place of the minimum surface tension.

Recently, a new approach to evaluate the quality of lung surfactant preparations beyond the γ_{min} value as the only quantitative characteristic has been developed [36]. This approach, called Compression–Relaxation Model (CRM), calculates the film properties independent of the compression protocol used.

Briefly, there are four obvious physical properties considered in this model: the elasticities of the film upon film compression and film expansion, an effective adsorption coefficient and an effective desorption coefficient. The elastic effects are quantified by standard surface thermodynamic definitions and the kinetic effects by standard first order kinetic equations. The combination of these four equations represents the Compression–Relaxation Model (CRM). The best fit of CRM to experimental dynamic surface tension data is sought by multi-variable optimization of the four elastic and kinetic constants and thus determines these four constants. A special feature of the model is its ability to account for the surface tension changes due to simultaneous changes of more than one of these parameters, e.g. elasticity of compression and desorption, at the same time.

Elasticity of the surfactant film gives an indication of how much area compression is needed to reduce the surface tension; in other words, higher elasticity indicates that less work is needed for breathing. Adsorption and relaxation indicate how fast the surfactant films are formed and how stable they are.

The dynamic behavior of lung surfactants plays an important role in the performance of these formulations. For example, the group of Hall has proposed a “super-compression" model [37] to explain the fact that fast compressions produce better dynamic surface tension response than slow compressions. CRM can be used as a tool to quantify these and other dynamic effects. Examples are the adsorption dynamics that was discussed previously [34,38] but has not been quantified in a systematic manner to compare various surfactant preparations, or the effect of additives and surfactant inhibitors.

In this paper, ADSA–CSD is used to measure the dynamic surface tension of a lung surfactant preparation, BLES, at concentrations, compression ratios and compression rates relevant to current exogenous surfactant therapies. The results are analyzed using CRM to evaluate the effect of surfactant concentration, compression ratio and compression rate on the surface activity and dynamic properties (elasticity, adsorption and relaxation) of BLES preparations. Results show that CRM is generally sensitive to all the parameters, i.e., elasticity, adsorption and relaxation, at any concentration at physiological conditions of 20% compression and 3 s per cycle. The model is also very sensitive to all the parameters at any concentration at low compression ratios and high frequency cycling. These latter conditions are relevant to the clinical practice of high frequency ventilation.

It will be shown that CRM has the ability to fit the surface tension response closely for a wide variety of parameters (compression ratio, compression rate and surfactant concentration) and produce sensible values for the elastic and kinetic parameters.

The key conclusion is that the four properties above are the determinant quantities for these systems.

2. Materials and experimental methods

2.1. Materials

The lung surfactant used, Bovine Lipid Extract Surfactant (BLES), was provided by BLES Biochemicals Inc. (London, Ontario, Canada) at a concentration of 27 mg/ml and was used without further treatment. BLES was divided into 1 ml glass vials in Ar atmosphere and

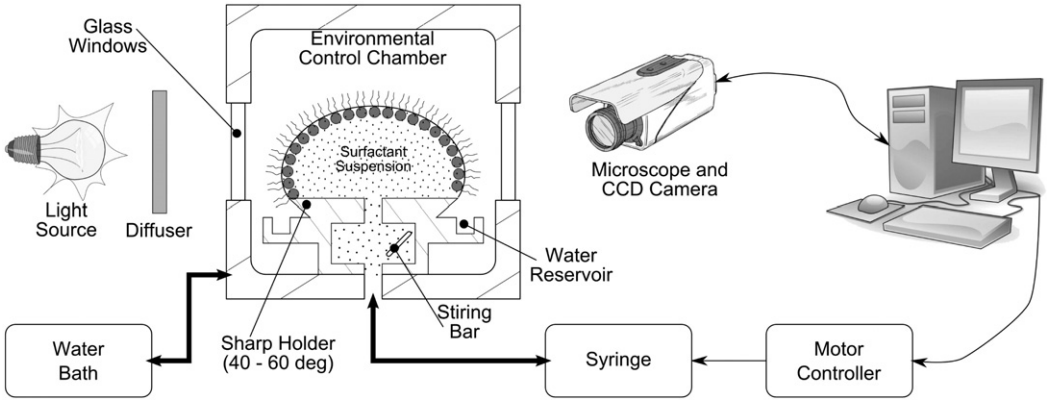

Fig. 1. A schematic diagram of the Axisymmetric Drop Shape Analysis–Constrained Sessile Drop (ADSA–CSD) experimental setup.

stored at −20 °C. On the day of the experiment, a vial was maintained at 37.5 °C water bath for 1 h before diluting it to the required concentration (2, 8, 15, or 27 mg/ml) in a salt solution of 0.6% NaCl and 1.5 mM $CaCl_2$. The pH value of the diluted BLES preparations ranged from 5 to 6.

2.2. Experimental procedure

The details of the design and operation of the surface tension technique, ADSA–CSD, were described elsewhere [25,34,10]. A schematic diagram of the ADSA–CSD setup is shown in Fig. 1. During the experiment, the setup is enclosed in an environmental control chamber that facilitates the control of gas composition and temperature. The humidity inside the chamber was kept constant at 100% relative humidity at 37 °C. The humid air is generated by filling the humidity control reservoir with distilled water one hour before the experiment to ensure that the chamber becomes saturated with water vapor, i.e. the relative humidity (RH) is ~100%.

A stepping motor (controller 18705/6, Oriel Instruments, Stratford, CT) was used to facilitate the fluid volume injection/withdrawal and the compression/expansion during the dynamic cycling part of the experiment. A CCD camera (model 4815-5000, Cohu Corp., Poway, CA) mounted on a horizontal microscope (type 400076, Wild Heerburgg, Switzerland) was used to acquire images throughout the experiment at a rate of 20 images per second for cycling speeds of 3 or 9 s per cycle and at a rate of 30 images per second for a cycling speed of 1 s per cycle. The images were digitized using a digital video frame grabber (Snapper-8, Active Silicon Ltd., Iver, UK) and stored in a workstation (SunBlade 1500, Sun Microsystems, Santa Clara, CA) for further analysis by ADSA (Axisymmetric Drop Shape Analysis). The system temperature is thermostatically maintained at 37 ± 0.2 °C by a water bath (Model RTE-111, Neslab Instruments Inc., Portsmouth, NH). The entire experimental setup, except the computer and water bath, is mounted on a vibration-free table (Technical Manufacturing Corp., Peabody, MA).

The experimental procedure is as follows: First, the sessile drop was quickly formed (within 0.5 s) on the pedestal. The drop is then left undisturbed to allow adsorption of the lung surfactant film. The surface tension is tracked until the film reaches the equilibrium surface tension (within 180 s for all cases). Thereafter, dynamic cycling is performed by successive compression/expansion of the drop. This is normally done through 20 cycles with the required periodicity (1, 3, or 9 per cycle) and the required compression ratio (percentage of surface area reduction) of 10%, 20%, or 30%. During every experimental run, images are acquired, stored and later analyzed with ADSA.

ADSA is a technique for measuring surface tension by matching an extracted drop profile to a theoretical one. Other outputs of ADSA are drop surface area, drop volume and radius of curvature at the drop apex [39–41].

All experiments were reproduced at least in triplicate. A typical experimental result for 2.0 mg/ml BLES at 100% relative humidity, 20% compression, 3 s per cycle and 37 °C is shown in Fig. 2 showing an example of ADSA outputs as a function of cycling time. It can be seen that cycles repeat very well.

2.3. CRM calculations

Using the change of surface tension and area with time during dynamic cycling, dynamic parameters are calculated using a compression–relaxation model (CRM). This model was introduced and described previously [36]. Briefly, in this model, there are four factors that affect the response of the dynamic surface tension: adsorption or spreading, desorption or relaxation, elasticity during compression and elasticity during expansion.

In CRM, the adsorption and relaxation rates are assumed to depend on the difference between the instantaneous surface tension and the equilibrium value, while the elasticity for both compression and expansion is assumed to depend on rate of change of the surface area of the interface. The main feature of CRM is the ability to account for the surface tension changes due to simultaneous changes of these parameters. This is different from other models that account for surface tension changes in different regions of a specific dominating parameter, but not allowing the various effects to occur simultaneously.

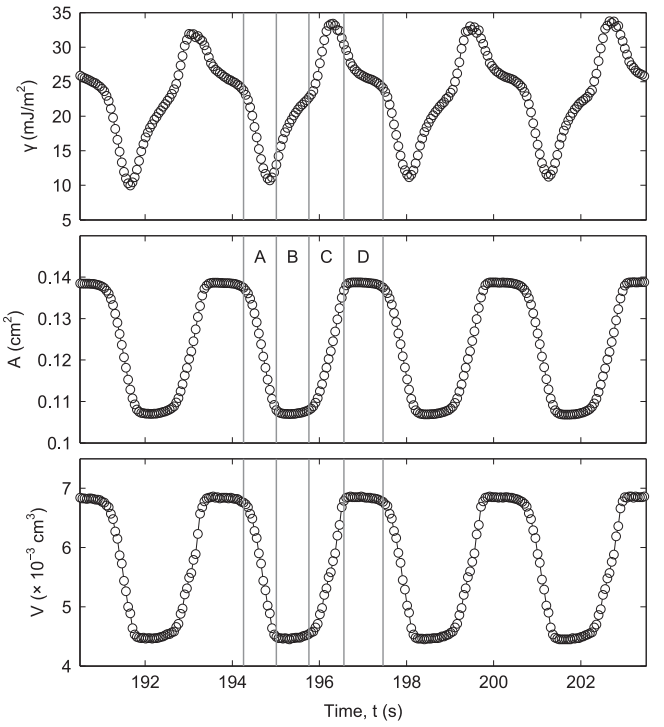

Fig. 2. The change of surface tension and surface area with time of 1 cycle for 2.0 mg/ml BLES at wet conditions (100% R.H.), 37 °C, and 20% compression ratio with a periodicity of 3 s per cycle.

Allowing the surface tension to change due to simultaneous effects of relaxation/adsorption and elasticity, CRM is described by the following set of equations [36]:

$$\frac{d\gamma}{dt} = \begin{cases} \frac{d\gamma_1}{dt} + \frac{d\gamma_2}{dt} & \text{if } \gamma \geq \gamma_{min} \\ 0 & \text{if } \gamma \leq \gamma_{min} \end{cases} \tag{1a}$$

where

$$\frac{d\gamma_1}{dt} = \begin{cases} k_a\left(\gamma_{eq} - \gamma\right) & \text{if } \gamma \geq \gamma_{eq} \\ k_r\left(\gamma_{eq} - \gamma\right) & \text{if } \gamma \leq \gamma_{eq} \end{cases} \tag{1b}$$

$$\frac{d\gamma_2}{dt} = \begin{cases} \epsilon_c\left(\frac{1}{A}\frac{dA}{dt}\right) & \text{if } \frac{dA}{dt} \leq 0 \\ \epsilon_e\left(\frac{1}{A}\frac{dA}{dt}\right) & \text{if } \frac{dA}{dt} \geq 0 \end{cases} \tag{1c}$$

Desirable dynamic properties of a good lung surfactant preparation are: fast adsorption rate (high k_a), slow relaxation rate (low k_r), and high elasticity of compression and expansion (high ϵ_c and ϵ_e). It should be noted that the rate constants are comparable only for the same compression rate.

Following convention [42,43], the elasticity used here is defined as:

$$\epsilon = \left|\frac{d\pi}{d\ln A}\right| = \left|\frac{d(\gamma_o - \gamma)}{dA/A}\right| \tag{2}$$

It refers to the dilatational elastic modulus of the surfactant film at the interface. For a two-dimensional interface, the stress is the surface pressure and the strain is the change of surface area per unit area. This corresponds to the bulk modulus in three dimensions.

The compression/relaxation model (CRM), as summarized in Eq. (3), is able to predict the surface tension response of a surfactant preparation, for given dynamic parameters. An initial value problem solver for ordinary differential equation is used for the numerical integration assuming an a priori knowledge of the above mentioned four dynamic parameters, namely adsorption coefficient (k_a), desorption coefficient (k_r), elasticity of compression ($_c$), and elasticity of expansion ($_e$). Conversely, for a given experimental condition, the values of these four parameters are optimized so that the calculated surface tension response fits best that of the experimentally measured surface tension response.

Details of the numerical methods used to obtain these four parameters for any experimental result were presented elsewhere [36]. Briefly, an initial guess procedure is used to quickly analyze the experimental result and calculate approximate values for the dynamic parameters. A dedicated integration module [44] is used to generate a surface tension response based on these calculated dynamic parameters using Eq. (1). A curve fitting module [45] is responsible for comparing the calculated surface tension values with the experimentally measured values, and modifying the parameter values until a matched surface tension response is obtained using a dedicated optimization procedure.

It is important to note that only one common value is used as the initial guess for both the elasticity of compression ($_c$) and the elasticity of expansion ($_e$). Physically, both parameters would be the same if the film had the same composition during compression and expansion. This point has been discussed in detail elsewhere [36].

3. Results

The dynamic cycling for a specific concentration is performed by successive compression/expansion of the drop. This is normally done through 20 cycles with the prescribed periodicity and the preselected compression ratio (percentage of surface area reduction). In this paper, 36 experiments are reported: 4 concentrations (2, 8, 15, or 27 mg/ml), 3 periodicities (1, 3, or 9 s per cycle), and 3 compression ratios (10%, 20%, or 30%); each experimental run contains 20 cycles and is repeated at least 3 times. In total, 108 runs were performed.

During every experimental run, images are acquired continuously at a rate of 30 images per second (for periodicity of 1 s per cycle) or 20 images per second (for periodicities of 3 and 9 s per cycle). A typical run contains approximately 600 images (20 cycles, 1 s per cycle and 30 images per second), 1200 images (20 cycles, 3 s per cycle and 20 images per second) or 3600 images (20 cycles, 9 s per cycle and 20 images per second). Thus, results reported here rely on almost 200,000 individual surface tension measurements, involving the analysis of that number of drop images. These images are stored and later analyzed with ADSA. For every image, ADSA calculates the surface tension, the surface area, and the drop volume as shown in Fig. 2. The reproducibility between cycles is apparent from Fig. 2.

The minimum value for surface tension for every cycle can be obtained by inspection from the output of ADSA. A typical run includes 20 values for the minimum surface tension. The reported minimum surface tension value is the average value within a particular run. For a specific condition (concentration, compression ratio, and compression rate), at least three runs were performed. From every run, an average minimum surface tension is reported in Fig. 3.

Fig. 3 shows the average minimum surface tension, γ_{min}, measured for four different concentrations of BLES (2, 8, 15, 27 mg/ml) at different compression ratios (10%, 20%, 30%) and different cycling conditions (1, 3, 9 s/cycle). The standard deviation indicated by the error bars shows good reproducibility between runs repeated under the same conditions.

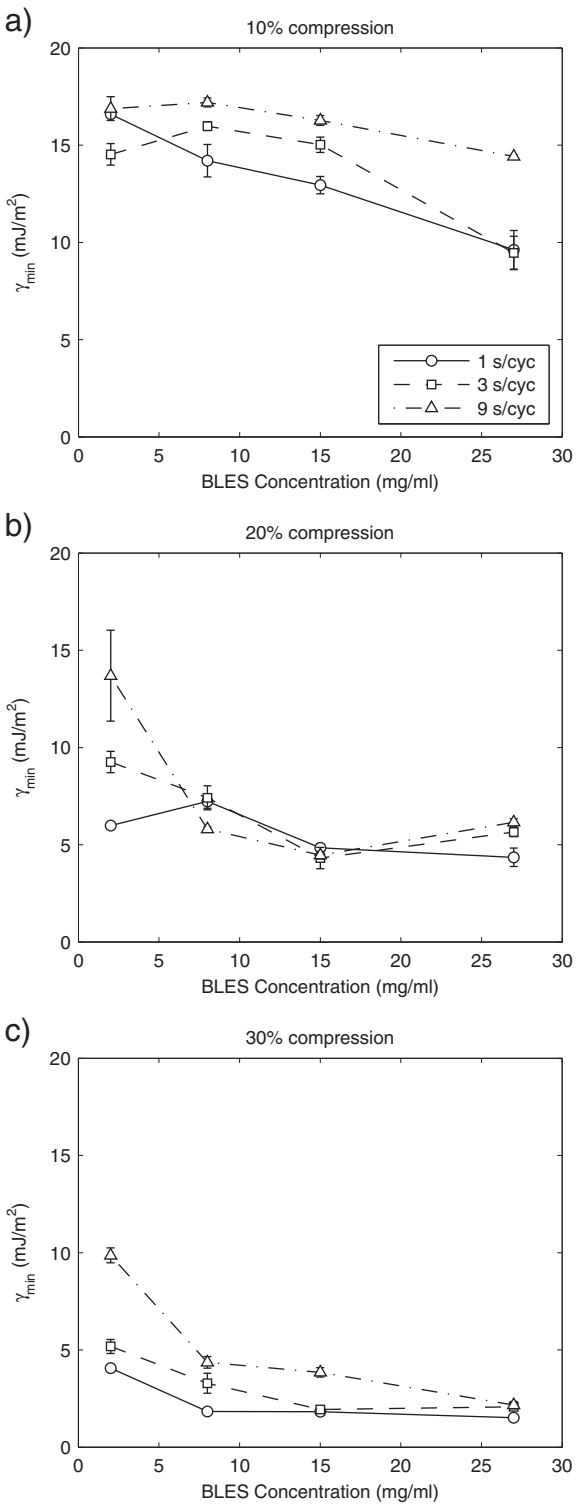

Fig. 3. The minimum surface tension, γ_{min}, measured for four different concentrations of BLES (2, 8, 15, 27 mg/ml) at different compression ratios (10%, 20%, 30%) and different cycling conditions (1, 3, 9 s/cycle). The error bars indicate the standard deviation between runs repeated under the same conditions.

At higher concentration, the minimum surface tension is sensitive to changes in periodicity only at small compression ratios. At 10% compression, the minimum surface tension decreases with the increase of concentration and with the increase of cycling rate. For 20% compression and above, the minimum surface tension decreases in the range of 2 mg/ml to 8 mg/ml but stays essentially constant at higher concentrations.

However, for concentrations above 8 mg/ml, there is no significant change in minimum surface tension. In clinical practice, high concentration BLES of 27 mg/ml is used [1,8]. and it is believed to be diluted after delivery to the lungs to a concentration close to 8 mg/ml [46,9,47–52].

Generally, increasing the extent of compression produces lower minimum surface tension values. This agrees with previous investigations of BLES at 0.5 and 5 mg/ml and cycling speeds of 3 and 10 s per cycle [10]. At high concentrations, the speed of cycling does not have a significant effect on the minimum surface tension. The decrease of minimum surface tension with the increase of the speed of compression at low concentrations agrees with previous investigations in the literature of BLES 0.5 mg/ml and 20% compression [10]. This dependence of minimum surface tension on speed is probably due to the fact that the speed of compression seems to be fast enough to prevent, in part, the hydration of the surfactant film [10].

It is important to note that ADSA–CSD studies can be performed readily at high rates of compression (to mimic human breathing at 3 s per cycle). In this study, higher rates are also reported (up to 1 s per cycle or 1 Hz). Even higher rates of compression are achievable after hardware upgrades for both the liquid control and image acquisition systems. It is noted that flow conditions and bulk viscosity might introduce errors in the measurement of surface tension via drop/shape methods when the cycling frequencies are 10 Hz or larger [53–55]. Therefore, an upper limit of 10 Hz exists for the high frequency studies. Our experiments are well below this limit so that it is safe to neglect the effect of bulk viscosity.

So far we have only considered the minimum surface tension value obtained at different conditions. While this minimum value may well be a useful indication of the response of that preparation to certain external conditions such as concentration, compression rate and ratio, it does not give a deeper understanding of the role neither of macroscopic effects like film elasticity nor microscopic or molecular effects such as effective adsorption coefficient of the film forming molecular species. It is the purpose of the Compression–Relaxation Model (CRM) to provide such insight.

Using the output of ADSA for every experimental run, the change of surface tension and surface area with time are analyzed using CRM following the procedure explained in Section 2.3. As mentioned earlier, a typical experimental run consists of 20 cycles. From every cycle, the four dynamic parameters of CRM are evaluated, i.e. elasticity of compression ($_c$), elasticity of expansion ($_e$), desorption/relaxation coefficient (k_r), and adsorption coefficient (k_a). An indication of the goodness of fit is also calculated for every cycle. The goodness of fit is defined below in Eq. (3), indicating the relative error between the predicted surface tension response from CRM and the experimentally measured surface tension response. Smaller values for the goodness of fit indicate a better fit.

Figs. 4 and 5 show sample experimental results of the change in surface tension with time and with relative surface area during dynamic cycling. Fig. 4 shows results of BLES concentrations 2 and 27 mg/ml at 10% compression and periodicities of 1 and 9 s per cycle. Fig. 5 shows corresponding results at 30% compression. The figures illustrate the quality, or "goodness of fit" of CRM to the experimental data. In these figures, the symbols represent the measured experimental results and the continuous lines represent the best-fit CRM curves, the four parameters ($_c$, $_e$, k_r, and k_a) determined from the experimental points having been used for the calculation of CRM curves.

Generally, results shown in Figs. 4 and 5 show that CRM fits almost all experimental conditions (high and low concentrations, cycling rates and compression ratios) very well. It can be concluded that the model using only four adjustable parameters is capable of capturing the features of the dynamic cycling for different conditions. However, there is a slight inconsistency between the model and the experimental results at the high surface tension range in some cases, e.g. Fig. 5(b) and (d). This disagreement only appears at the highest compression ratio (30%) and the lowest compression rates (9 s per cycle). In these cases, the compression is slow, and hence the details of the adsorption and elasticity effects are pronounced near the highest surface tension values. As the area is increased, the surface tension increases due to the film elasticity; however, if the surface tension exceeds the equilibrium value, the surface tension tends to decrease at the same time due to adsorption to the interface. Since the compression is slow in these cases, the surface tension shows some fluctuations near the highest surface tension range. The adsorption in such cases is much quicker than the speed of compression, causing these fluctuations to be very pronounced. Such low compression rates are not really relevant clinically; however, this lack of agreement is considered in more detail below.

The same procedure of extracting the dynamic parameters from every cycle is applied for all 20 cycles in every experimental run. An effective value for each of the parameters is formed by the multi-variable optimization for every cycle. 20 values for each of the four dynamic parameters and the goodness of fit are calculated for every run. From every run, average values are calculated. For a specific condition (concentration, compression ratio, and compression rate), at least three runs were performed. For each of the 36 different experimental conditions considered, the values of the goodness of fit and the four dynamic parameters reported below in Figs. 6 to 10 are the average values of the parameter plotted on the ordinate across repeated runs and the 95% confidence limit.

The visual judgment of a good fit between experimental points and calculated curves can be quantified by means of a "goodness of fit". Fig. 6 compares the values of the goodness of fit from CRM calculated at different experimental conditions. The goodness of fit is defined as:

$$GF = \sqrt{\sum \left| \frac{\gamma_e - \gamma_m}{\gamma_e} \right|^2} \tag{3}$$

where γ_e is the experimentally measured surface tension value and γ_m is the predicted surface tension value from CRM. Smaller values for the goodness of fit indicate a better fit. It turns out that CRM fits almost all experimental conditions (high and low concentrations, cycling rates and compression ratios) very well except for a few points at higher compression ratios. The best results for the goodness of fit are at any concentration at low compression ratios and high frequency cycling. These conditions are relevant to clinical practice of high frequency ventilation. The goodness of fit gives an indication of the conditions where CRM works best. This point of the applicability of the model to certain conditions is considered in more detail below.

Figs. 7 and 9 show the calculated elasticity of compression, $_c$, and elasticity of expansion, $_e$, obtained at different experimental conditions. Figs. 8 and 10 show the calculated relaxation coefficient, k_r, and adsorption coefficient, k_a, obtained at different experimental conditions. A detailed inspection of every parameter will follow below. In these four figures, the values reported are the average values across repeated runs and the 95% confidence limit. Asterisks are used in these figures to highlight points where CRM is less sensitive to one or more of the parameters. The quantification of the sensitivity of the model is described in Section 4.2.

4. Discussion

4.1. Dynamic CRM parameters

The change of the elasticity of compression, $_c$, with concentration, compression ratio and compression rate is shown in Fig. 7. It is expected that the elasticity is an intrinsic property of the lung surfactant preparation that should not change with different experimental conditions. The elasticity of compression did indeed remain almost the same with concentration beyond 8 mg/ml. There is also no significant change with compression ratio or compression rate. This agrees with previous studies

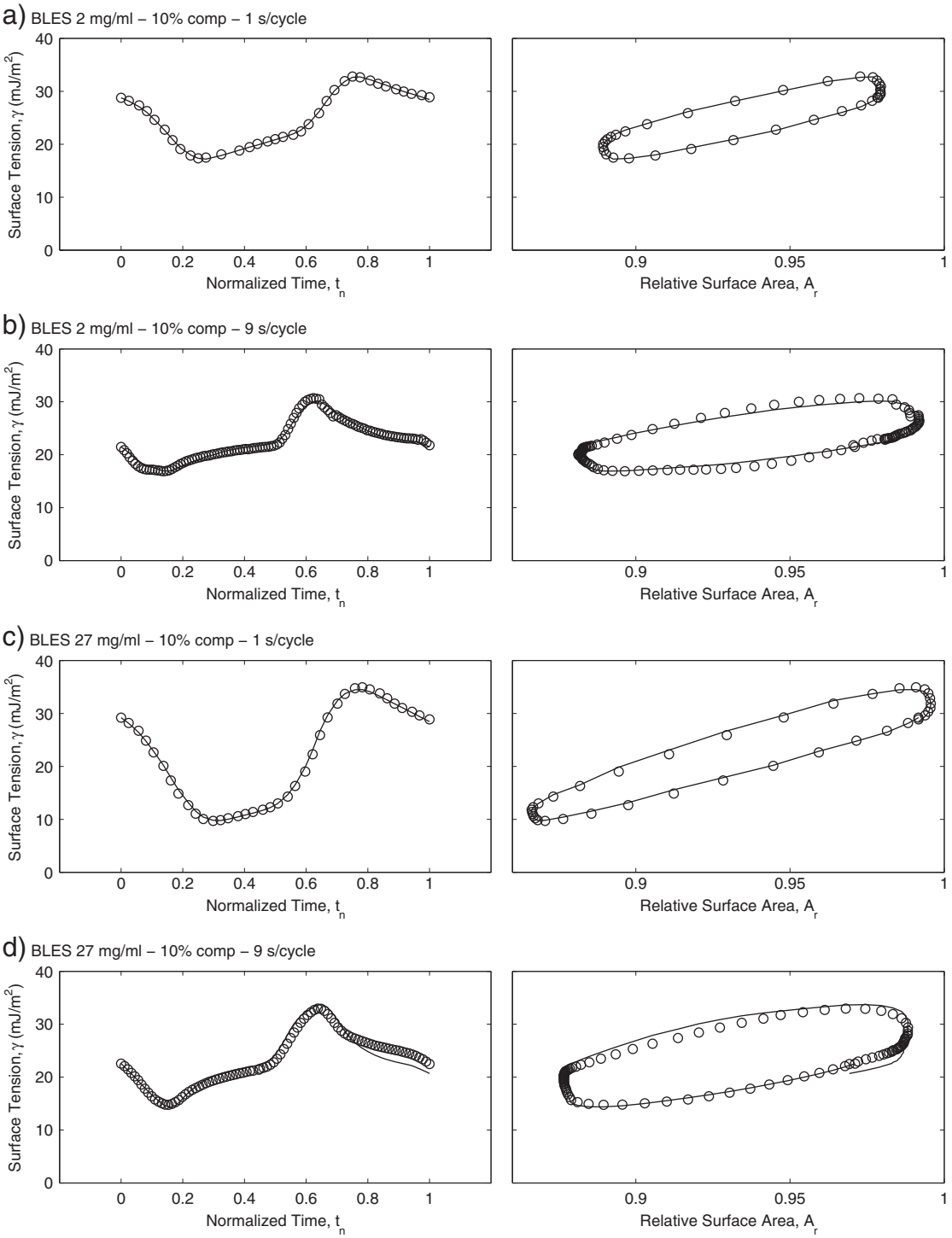

Fig. 4. The change in surface tension with time and with relative surface area during dynamic cycling of BLES at 10% compression and different concentrations and periodicities: (a) 2 mg/ml and 1 s/cycle; (b) 2 mg/ml and 9 s/cycle; (c) 27 mg/ml and 1 s/cycle; (d) 27 mg/ml and 9 s/cycle. Symbols show the measured surface tension values and lines show the values predicted from CRM.

on BLES with concentrations 0.5 and 2 mg/ml at 20% compression and 3 s per cycle [36]. In previous studies of DPPC spread films at compression ratios between 0.1 and 30% and frequencies 0.02, 0.05 and 0.1 Hz, the dilatational elasticities were found to be almost constant for compression ratios higher than 1% and for all frequencies studied [56]. Spread films of of n-dodecyl dimethyl phosphine oxide ($DC_{12}PO$), at compression ratios in the range of 2% to 10% and frequencies in the range of 0.015 to 0.57 Hz, did not show significant change in the dilatational elasticities [57].

Elasticity of compression of BLES was previously evaluated using an elementary procedure [10]. The surface tension–relative area curve during the compression stage was fitted to a fourth order polynomial equation, and the first derivative was used to calculate the dilatational elasticity at the midpoint of the compression. Using this elementary procedure with the current data of BLES 2 mg/ml, 20% compression and 3 s/cycle produces values for the elasticity of compression around 100 mJ/m^2, while values calculated here are between 130 and 140 mJ/m^2. Therefore, the elasticity of compression values are

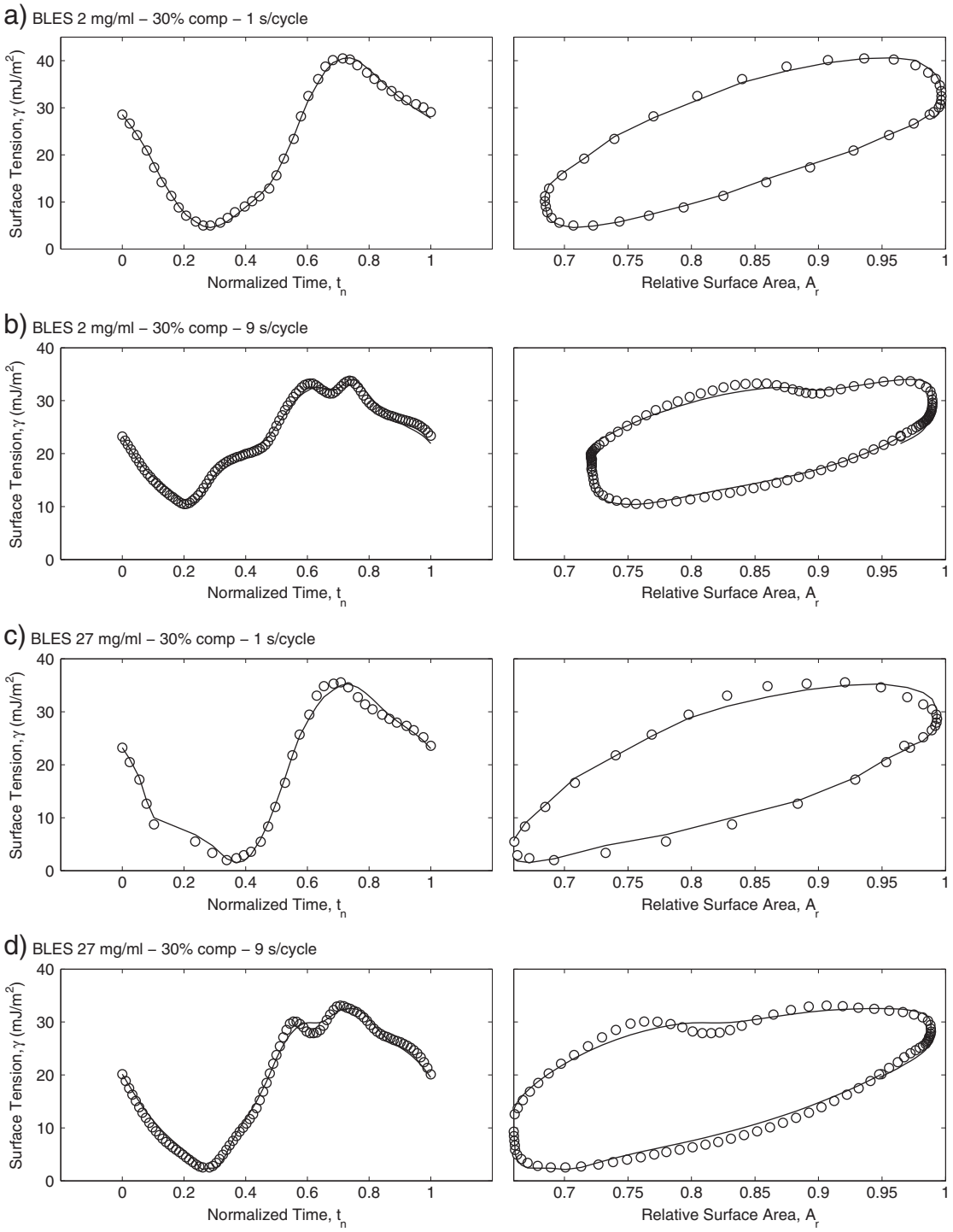

Fig. 5. The change in surface tension with time and with relative surface area during dynamic cycling of BLES at 30% compression and different concentrations and periodicities: (a) 2 mg/ml and 1 s/cycle; (b) 2 mg/ml and 9 s/cycle; (c) 27 mg/ml and 1 s/cycle; (d) 27 mg/ml and 9 s/cycle. Symbols show the measured surface tension values and lines show the values predicted from CRM.

underestimated by about 30% if that elementary procedure [10] is used. The same effect exists for other experiments at different conditions. The reason for this is the role of desorption: The elementary procedure assumes that the elasticity is the only active physical phenomenon during the film compression neglecting any effects of desorption/relaxation. On the other hand, CRM accounts for simultaneous effects of elasticity and relaxation during the film compression. The relaxation causes an increase in the surface tension during compression especially in humid conditions, and that increase becomes larger as the film is compressed as explained in Eq. (1b). Therefore, neglecting relaxation causes the elasticity of compression to be underestimated.

Other studies of DPPC/SP-B, DPPC/SP-C, DPPC/SP-B/SP-C spread films did not show any dependence of the elasticity on the compression speed [58–60,35]. These results support the concept that more flexible film structures are formed in the presence of surfactant proteins [61]. It can be concluded that the elasticity parameter in CRM is a property of the lung surfactant preparation. In fact, the addition of an inhibitor,

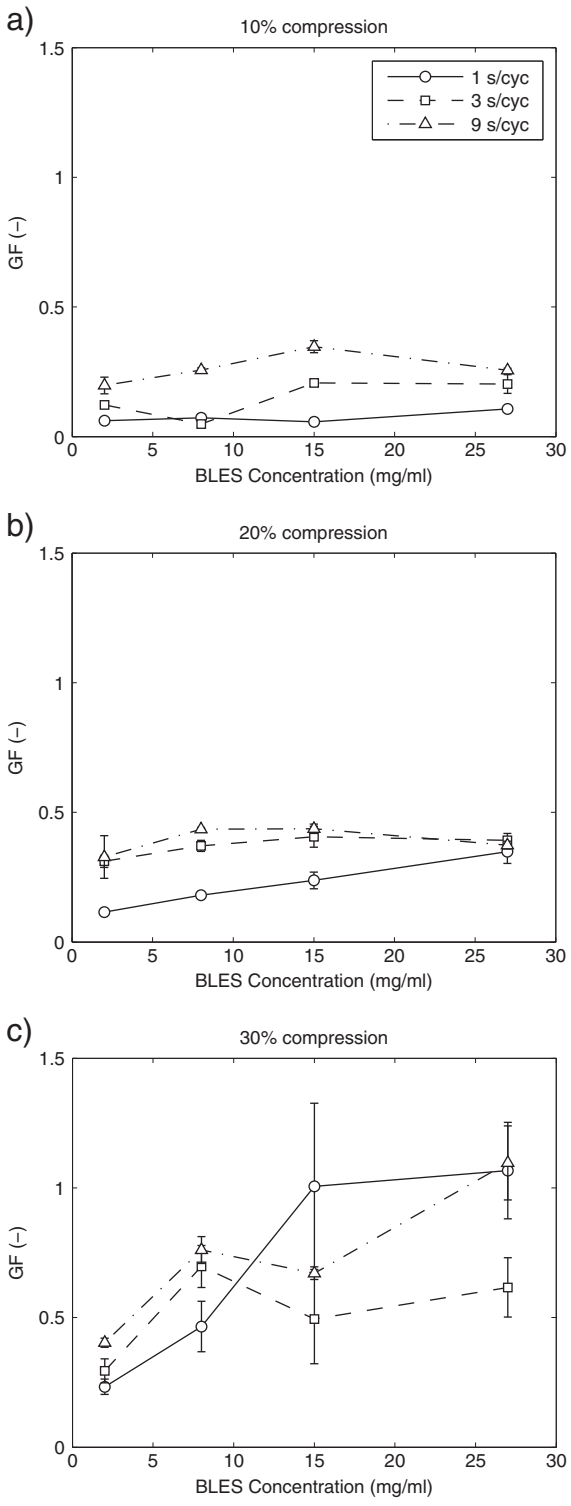

Fig. 6. The goodness of fit for CRM measured for four different concentrations of BLES (2, 8, 15, 27 mg/ml) at different compression ratios (10%, 20%, 30%) and different cycling conditions (1, 3, 9 s/cycle). The error bars indicate the standard deviation between runs repeated under the same conditions.

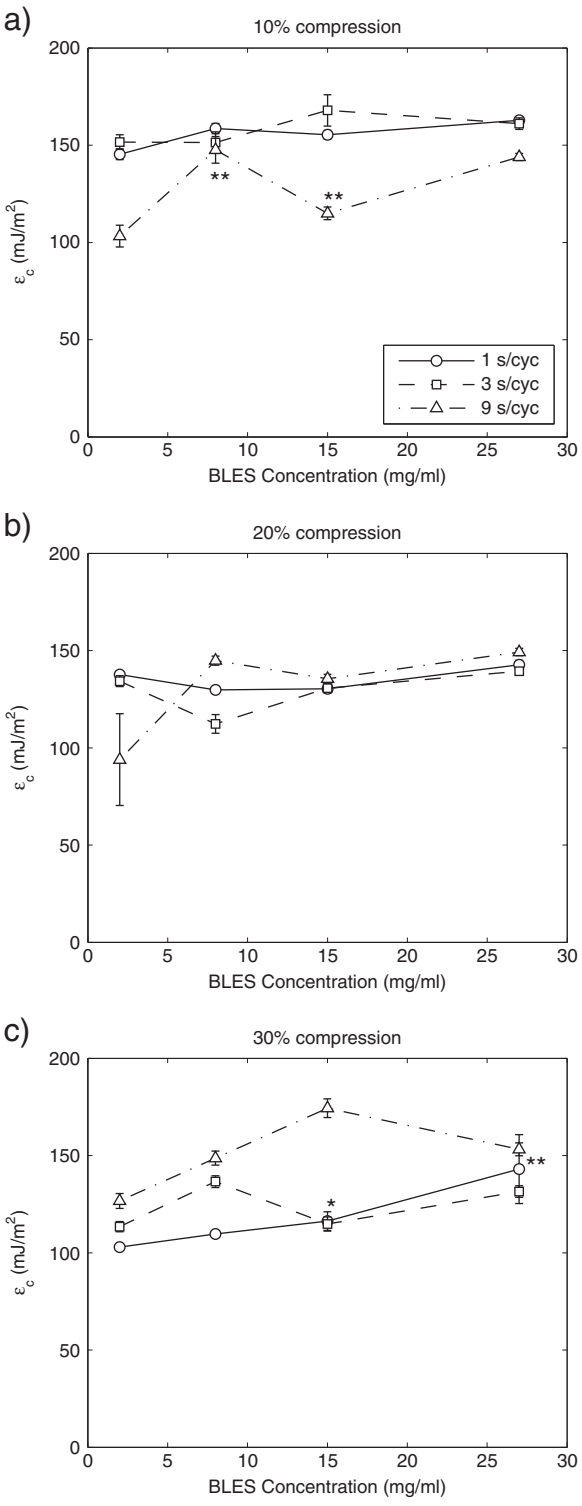

Fig. 7. The elasticity of compression, ε_c, calculated from CRM for four different concentrations of BLES (2, 8, 15, 27 mg/ml) at different compression ratios (10%, 20%, 30%) and different cycling conditions (1, 3, 9 s/cycle). The asterisks show the range of insensitivity (explained in Fig. 12): * indicate points with range of insensitivity bigger than 0.2, ** indicate points with range of insensitivity bigger than 0.5.

e.g. serum, albumin, fibrinogen, or excess cholesterol, to lung surfactant preparations is known to significantly reduce the elasticity of compression of BLES [27].

The change of the relaxation coefficient, k_r, with concentration, compression ratio and compression rate is shown in Fig. 8. There is some variability but not a pronounced dependence on surfactant concentration.

There is no significant dependence on concentrations at all compression ratios or compression rates except for a few points at the 10% compression. There is a small increase in the relaxation coefficient when the compression ratio is increased from 20% to 30%. This agrees with published results for BLES [10].

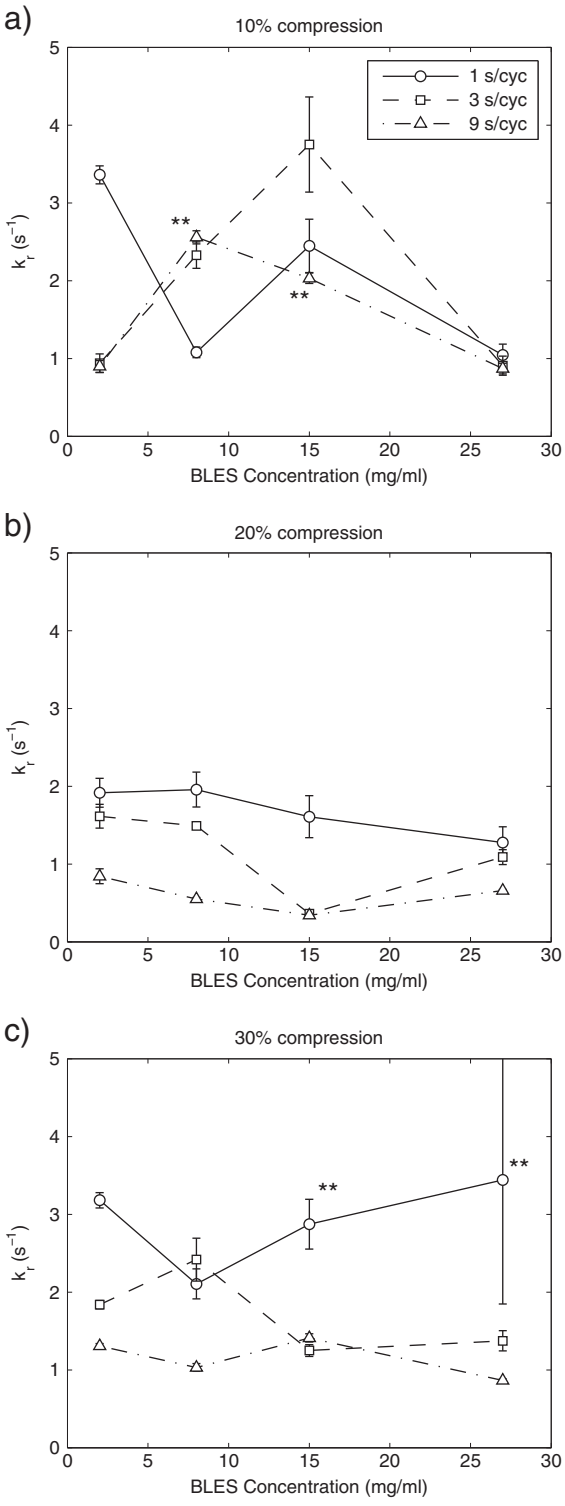

Fig. 8. The relaxation coefficient, k_r, calculated from CRM for four different concentrations of BLES (2, 8, 15, 27 mg/ml) at different compression ratios (10%, 20%, 30%) and different cycling conditions (1, 3, 9 s/cycle). The asterisks show the range of insensitivity (explained in Fig. 12): * indicate points with range of insensitivity bigger than 0.2, ** indicate points with range of insensitivity bigger than 0.5.

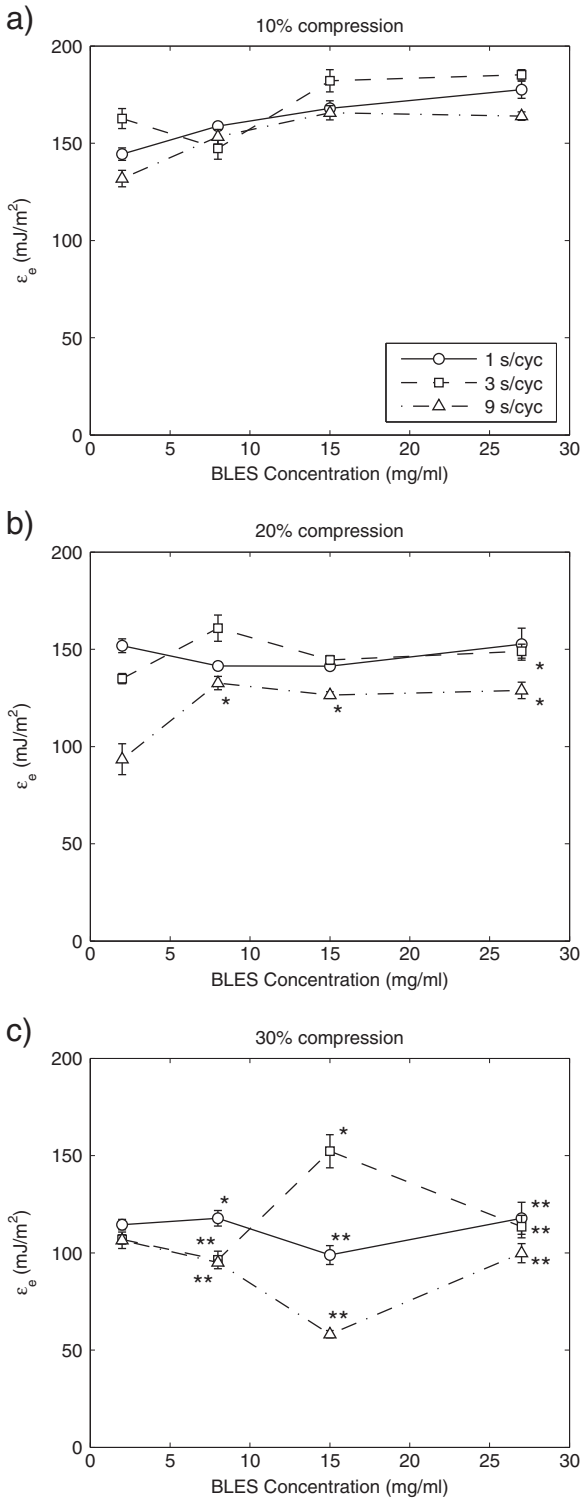

Fig. 9. The elasticity of expansion, ε_e, calculated from CRM for four different concentrations of BLES (2, 8, 15, 27 mg/ml) at different compression ratios (10%, 20%, 30%) and different cycling conditions (1, 3, 9 s/cycle). The asterisks show the range of insensitivity (explained in Fig. 12): * indicate points with range of insensitivity bigger than 0.2, ** indicate points with range of insensitivity bigger than 0.5.

The relaxation coefficient depends also on the speed of compression; the higher the frequency, the higher the relaxation coefficient. This agrees with other studies of BLES [10] and $DC_{12}PO$ [57].

It has to be kept in mind that the magnitude or extent of relaxation, i.e. the increase of surface tension with time, decreases with the increase of compression rate. This can be seen in Fig. 5. Fig. 5(a) shows the change of surface tension with relative surface area at a high compression rate (1 s/cycle) while Fig. 5(b) shows similar results at a lower compression rate (9 s/cycle). It is clear that the magnitude of surface tension relaxation is larger in the second case. The decrease in surface tension relaxation with increasing compression rate is consistent with previous work [10] and the trend expected from Hall's super-compression model [37]. The

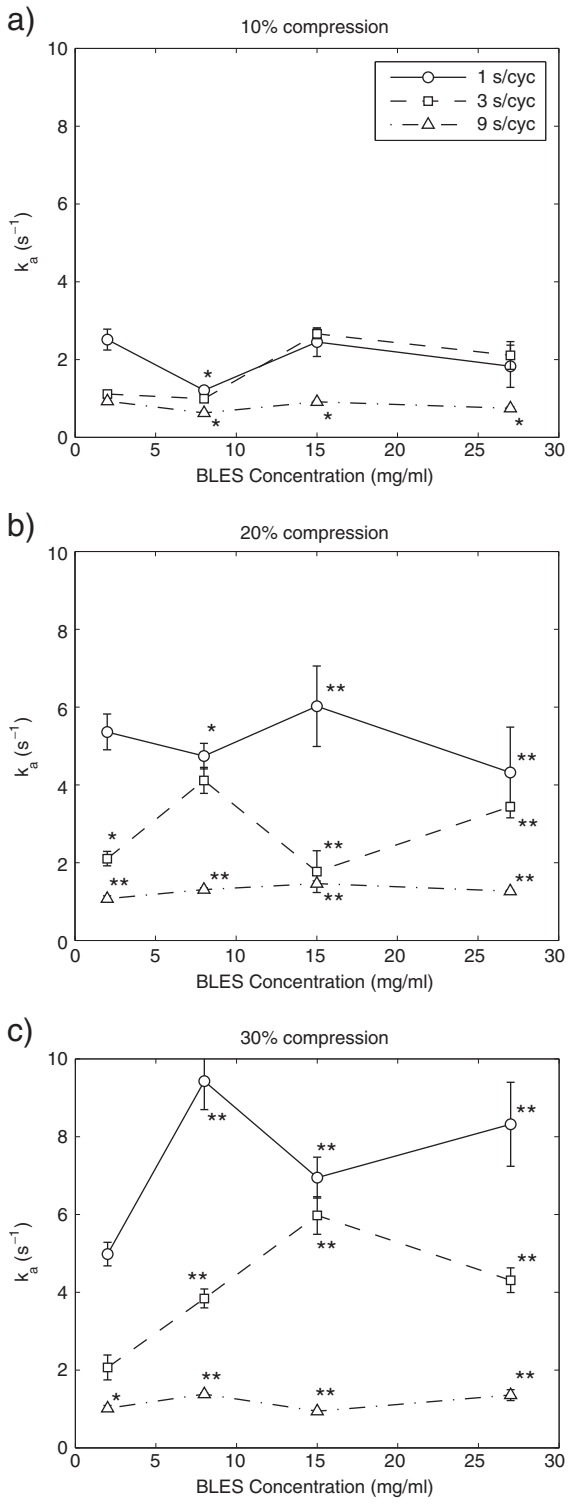

Fig. 10. The adsorption coefficient, k_a, calculated from CRM for four different concentrations of BLES (2, 8, 15, 27 mg/ml) at different compression ratios (10%, 20%, 30%) and different cycling conditions (1, 3, 9 s/cycle). The asterisks show the range of insensitivity (explained in Fig. 12): * indicate points with range of insensitivity bigger than 0.2, ** indicate points with range of insensitivity bigger than 0.5.

relationship between the magnitude of surface tension relaxation and the relaxation coefficient can be understood from Eq. (1b). For the same compression rate, the increase or decrease of the magnitude of surface tension relaxation will correspond to a similar change in the relaxation coefficient. However, for different compression rates, the relationship between the magnitude of surface tension relaxation and the relaxation coefficient will depend on the time available for relaxation; this time is generally shorter for higher compression rates. In analyzing the trends of the relaxation coefficients, it is also important to note that BLES does not have all the surfactant proteins of the original bovine surfactant. BLES is deficient in SP-B whose role is to stabilize the surfactant film [2]. Future studies using CRM framework should be conducted to explore these effects in more detail.

The change of the elasticity of expansion, $_e$, with concentration, compression ratio and compression rate is shown in Fig. 9. Values are very close to the elasticity of compression. Generally, there is no significant dependence on concentration, compression ratio or compression rate. However, the sensitivity of the model to changes in $_e$ of most experiments at 30% compression is low. This leads to less reliable values at these conditions.

The change of the adsorption coefficient, k_a, with concentration, compression ratio and compression rate is shown in Fig. 10. There is some variability but not a pronounced dependence on surfactant concentration. However, this variability is reproducible as indicated by the error bars in the figure. The adsorption coefficient seems to increase with the increase of the compression ratio and compression rate. However, the sensitivity of most points at 20% and 30% compression is very low. This leads to less reliable k_a values at these conditions. More details regarding the sensitivity of the model are given in Section 4.2.

4.2. Sensitivity of CRM

For some experiments reported here, it is noticed that the fitting of CRM to the experimental results are not sensitive to one or more of the four dynamic parameters. To further investigate this point, a detailed sensitivity study was performed. The details of calculating the "range of insensitivity" for each parameter is given in Appendix **A**. Briefly, it is attempted to identify for each parameter the range in which CRM is not highly sensitive. The sensitivity of the model (in terms of the goodness of fit) to changes in the respective parameter is calculated as the percentage change of the goodness of fit divided by the percentage change of the parameter. For example, a sensitivity of 1 means that a relative change of, say 20%, of a specific parameter yields a relative change of the same amount, 20% in this case, of the goodness of fit. A sensitivity cut-off level of 1 is chosen to differentiate between sensitive and insensitive values. The range of percentage change of the parameter in which the sensitivity of the model is below 1 is called here the "range of insensitivity" for a specific parameter. The procedure is applied for each of the four parameters of CRM and the range of insensitivity is calculated for each in all experiments. A summary of these calculations is shown in Fig. 11.

In this figure, the contour lines show the range of insensitivity for each parameter. Higher values indicate that the model is less sensitive to a wider range for this specific parameter. It can be seen that there are similarities between the insensitivity contours of both elasticity of compression and relaxation coefficient and also between both elasticity of expansion and adsorption coefficient.

From these contours, experimental conditions can be identified where CRM is less sensitive to certain parameters. Such information can be very useful as recommendations can be made to what experimental conditions are to be used if there is an interest in a specific parameter. For example, the elasticity of compression, $_c$, and the relaxation coefficient, k_r, are less sensitive at high concentrations, high compression ratios, and high cycling rates. The fit is also less sensitive to $_c$ and k_r at low compression ratios and low cycling rates; at these conditions the parameters $_e$ and k_a are more sensitive. The elasticity of expansion, $_e$, and the adsorption coefficient, k_a, are less sensitive at high concentrations and high compression ratios.

It is important to note that CRM is generally sensitive to all the parameters at any concentration at physiological conditions of 20% compression and 3 seconds per cycle. The model is also sensitive to all the parameters at any concentration at low compression ratios and high frequency

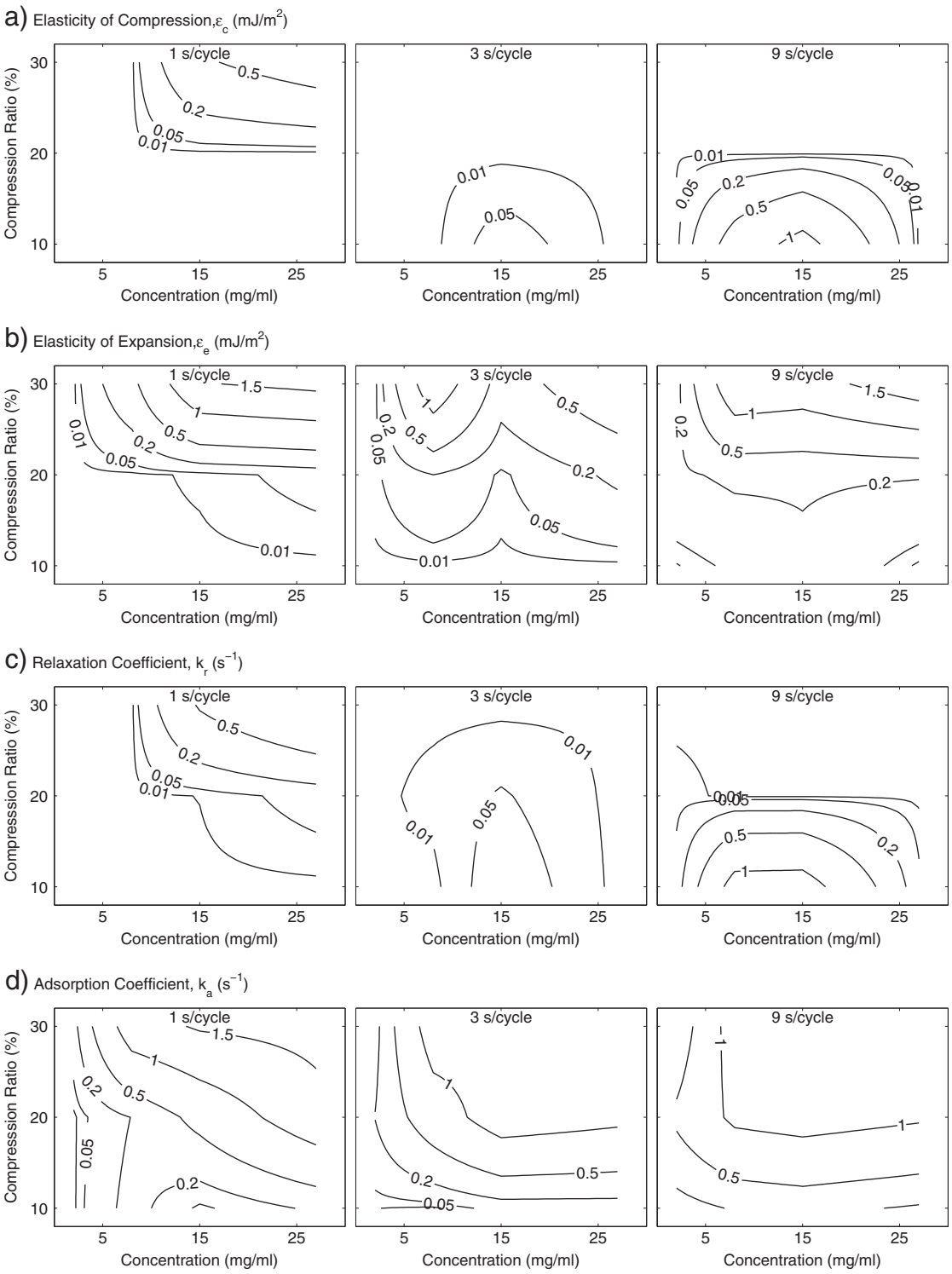

Fig. 11. Contour lines of the range of insensitivity for each of the parameters: (a) ε_c, (b) ε_e, (c) k_r, (d) k_a, at different periodicities, compression ratios and concentrations. The calculation of the range of insensitivity is explained in Fig. 12.

cycling. These conditions are relevant to conventional and high frequency ventilation.

Generally, the effect of the concentration on the four dynamic parameters is minimal beyond 8 mg/ml. We infer that such lung surfactant studies should generally be performed at concentrations if 8 mg/ml or higher, to guarantee clinical relevance. This is important for clinical therapeutic practice where it is believed that increased concentration will improve the surfactant properties. As shown here, increasing surfactant concentration does improve the dynamic properties only in the low concentration range below 8 mg/ml.

Although the dynamic properties of BLES-only preparations do not improve significantly with increasing BLES concentration, the same might not be true in the presence of inhibitors. For example, it was shown before [36] that when albumin is added to BLES, the elasticity value is markedly decreased indicating surfactant inactivation or inhibition. Using ADSA–CSD in combination with CRM, the effect of relevant additives and/or inhibitors

could be evaluated at appropriate conditions of concentration, compression rate and compression ratio.

Acknowledgments

We thank BLES Biochemicals Inc. for the generous donation of the BLES samples. This work is supported by a grant from Natural Sciences and Engineering Research Council (NSERC) of Canada (Grant No. 8278) and an open fellowship from University of Toronto as well as Ontario Graduate Scholarship to Sameh M. I. Saad.

Appendix A. Range of insensitivity

This appendix explains the calculations of the range of insensitivity for each parameter of CRM. First, the change of goodness of fit (defined in Eq. (3)) is recalculated after changing the respective parameter around the calculated value while keeping the rest of the parameters constant. Two examples are shown in Fig. 12(a) and (b) for one of the cycles of 2.0 mg/ml BLES at 20% compression ratio with a periodicity of 9 s per cycle. In Fig. 12(a), the change of goodness of fit is plotted versus the change of one of the parameters ($_c$) around the calculated value while keeping the rest of the parameters ($_e$, k_r, k_a) constant. In Fig. 12(b), the change of goodness of fit is plotted versus the change of one of the parameters (k_a) around the calculated value while keeping the rest of the parameters ($_c$, $_e$, k_r) constant.

The second step is to calculate the sensitivity of the model (in terms of the goodness of fit) to changes in the respective parameter by calculating the percentage change of the goodness of fit divided by the percentage change of the parameter. For example, for the case of the adsorption coefficient, k_a, the sensitivity of the model with respect to this parameter is,

$$S = \left| \frac{\Delta GF/GF}{\Delta k_a/k_a} \right| \tag{A.1}$$

Samples are shown in Fig. 12(c) and (d) for the same experiment. In these figure, the relative change of sensitivity is plotted versus the relative change of one of the parameters ($_c$ or k_a).

The third step is to define the "range of insensitivity" based on the sensitivity calculations. A cut-off level of 1 is chosen to differentiate between sensitive and insensitive values. If the change in the respective parameter yields a sensitivity more than 1, the model is considered sensitive to this parameter at this change level, and vice versa. Hence, the range of insensitivity for this parameter is defined as the range of percentage change of the parameter in which the sensitivity of the model is below 1.

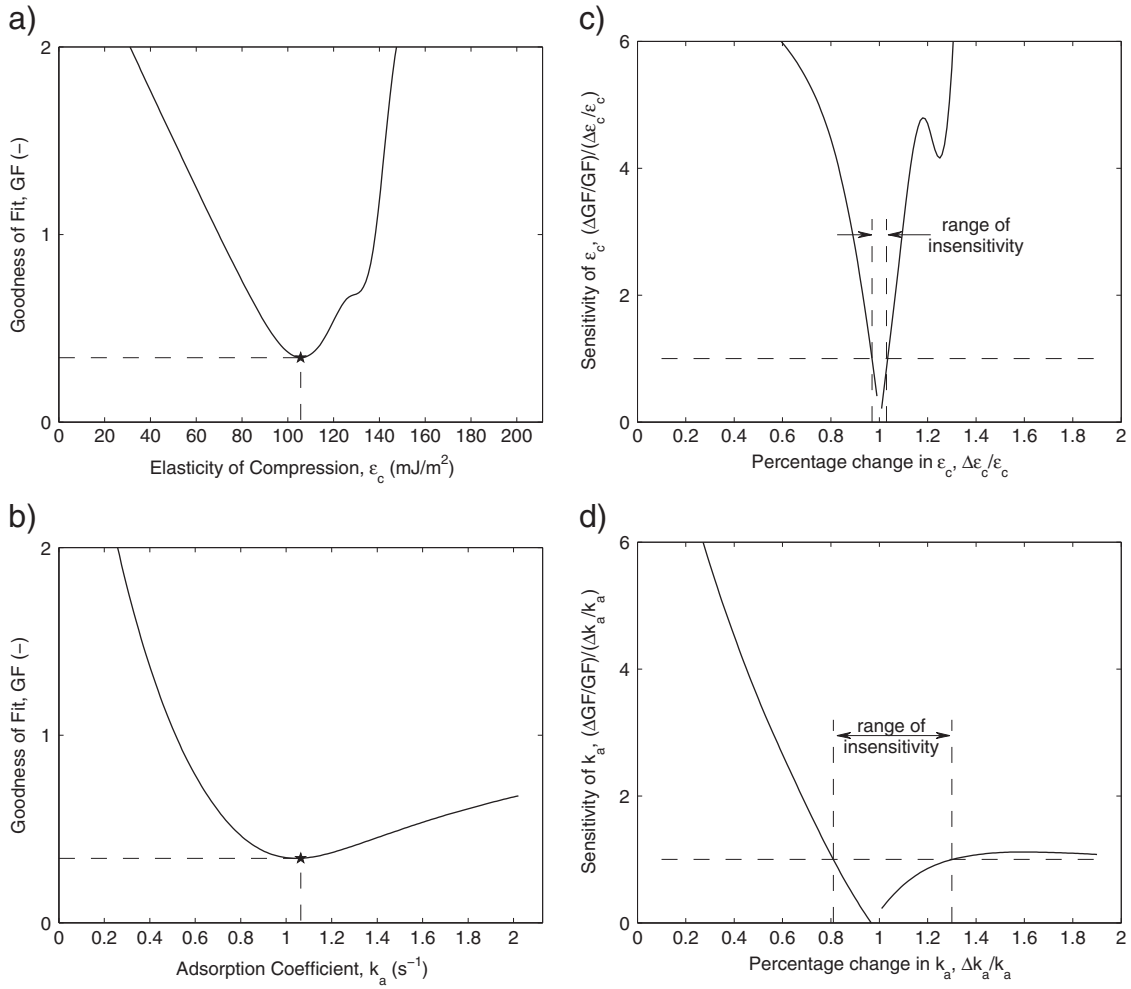

Fig. 12. Calculation of the range of insensitivity for the elasticity of the compression $_c$ and the adsorption coefficient k_a of one cycle for 2.0 mg/ml BLES at 20% compression ratio with a periodicity of 9**s** per cycle: (a) The change of goodness of fit with the change of $_c$ around the calculated value while keeping the rest of the parameters ($_e$, k_r, k_a) constant. (b) The change of goodness of fit with the change of k_a around the calculated value while keeping the rest of the parameters ($_c$, $_e$, k_r) constant. (c) The relative change of sensitivity with the relative change of $_c$. (d) The relative change of sensitivity with the relative change of k_a. The range of insensitivity is the range of percentage change of the parameter in which the sensitivity is below 1.

In our example of Fig. 12(c), CRM is found to be insensitive to small changes in this parameter, $_c$, in the range of roughly 98% to 102% of the calculated value for $_c$. This means that the range of insensitivity of the model to the parameter $_c$ is found to be 0.04 in this experiment as shown in the figure. In Fig. 12(d), CRM is found to be insensitive to small changes in this parameter, k_a, in the range of roughly 82% to 133% of the calculated value for k_a. This means that the range of insensitivity of the model to the parameter k_a is found to be 0.51 in this experiment as shown in the figure.

The same procedure is applied for each of the four parameters of CRM and the range of insensitivity is calculated for each in all the experiments. A summary of these calculations is shown in Fig. 11.

References

[1] R.H. Notter, Lung surfactants : basic science and clinical applications, Marcel Dekker, New York, 2000.
[2] Y.Y. Zuo, R.A.W. Veldhuizen, A.W. Neumann, N.O. Petersen, F. Possmayer, Current perspectives in pulmonary surfactant — inhibition, enhancement and evaluation, Biochim. Biophys. Acta - Biomembr. 1778 (10) (2008) 1947–1977.
[3] W.A. Engle, A.R. Stark, D.H. Adamkin, D.G. Batton, E.F. Bell, V.K. Bhutani, S.E. Denson, G.I. Martin, K.L. Watterberg, Surfactant-replacement therapy for respiratory distress in the preterm and term neonate, Pediatrics 121 (2) (2008) 419–432.
[4] I. Frerking, A. Gunther, W. Seeger, U. Pison, Pulmonary surfactant: functions, abnormalities and therapeutic options, Intensive Care Med. 27 (11) (2001) 1699–1717.
[5] J.F. Lewis, R. Veldhuizen, The role of exogenous surfactant in the treatment of acute lung injury, Annu. Rev. Physiol. 65 (2003) 613–642.
[6] J.J. Haitsma, P.J. Papadakos, B. Lachmann, Surfactant therapy for acute lung injury/acute respiratory distress syndrome, Curr. Opin. Crit. Care 10 (1) (2004) 18–22.
[7] J.F. Lewis, R.A.W. Veldhuizen, The future of surfactant therapy during ALI/ARDS, Semin. Respir. Crit. Care Med. 27 (4) (2006) 377–388.
[8] H.W. Taeusch, Treatment of acute (adult) respiratory distress syndrome. the holy grail of surfactant therapy, Biol. Neonate 77 (SUPPL. 1) (2000) 2–8.
[9] A.H. Jobe, Surfactant in the perinatal period, Early Hum. Dev. 29 (1–3) (1992) 57–62.
[10] E.J. Acosta, R. Gitiafroz, Y.Y. Zuo, Z. Policova, P.N. Cox, M.L. Hair, A.W. Neumann, Effect of humidity on lung surfactant films subjected to dynamic compression/expansion cycles, Respir. Physiol. Neurobiol. 155 (3) (2007) 255–267.
[11] C.S. Calfee, M.A. Matthay, Nonventilatory treatments for acute lung injury and ARDS, Chest 131 (3) (2007) 913–920.
[12] R. Jain, A. DalNogare, Pharmacological therapy for acute respiratory distress syndrome, Mayo Clin. Proc. 81 (2) (2006) 205–212.
[13] K.J. Bosma, J.F. Lewis, Emerging therapies for treatment of acute lung injury and acute respiratory distress syndrome, Expert Opin. Emerg. Drugs 12 (3) (2007) 461–477.
[14] M. Tidswell, Nonventilatory interventions in ALI/ARDS: recent work, J. Intensive Care Med. 23 (1) (2008) 70–72.
[15] R.G. Spragg, J.F. Lewis, W. Wurst, D. Hafner, R.P. Baughman, M.D. Wewers, J.J. Marsh, Treatment of acute respiratory distress syndrome with recombinant surfactant protein c surfactant, Am. J. Respir. Crit Care Med. 167 (11) (2003) 1562–1566.
[16] M.B.P. Amato, C.S.V. Barbas, D.M. Medeiros, R.B. Magaldi, G.D.P.P. Schettino, G. Lorenzi-Filho, R.A. Kairalla, D. Deheinzelin, C. Munoz, R. Oliveira, T.Y. Takagaki, C.R.R. Carvalho, Effect of a protective-ventilation strategy on mortality in the acute respiratory distress syndrome, N. Engl. J. Med. 338 (6) (1998) 347–354.
[17] R.G. Brower, M.A. Matthay, A. Morris, D. Schoenfeld, B.T. Thompson, A. Wheeler, Ventilation with lower tidal volumes as compared with traditional tidal volumes for acute lung injury and the acute respiratory distress syndrome, N. Engl. J. Med. 342 (18) (2000) 1301–1308.
[18] R.G. Brower, P.N. Lanken, N. MacIntyre, M.A. Matthay, A. Morris, M. Ancukiewicz, D. Schoenfeld, B.T. Thompson, Higher versus lower positive end-expiratory pressures in patients with the acute respiratory distress syndrome, N. Engl. J. Med. 351 (4) (2004) 327–336+411.
[19] A.J. Aspros, C.G. Coto, J.F. Lewis, R.A.W. Veldhuizen, High-frequency oscillation and surfactant treatment in an acid aspiration model, Can. J. Physiol. Pharmacol. 88 (1) (2010) 14–20.
[20] X. Wen, K.C. McGinnis, E.I. Franses, Unusually low dynamic surface tensions of aqueous solutions of sodium myristate, Colloids Surf., A Physicochem. Eng. Asp. 143 (2–3) (1998) 371–380.
[21] T.D. Graff, D.W. Benson, Systemic and pulmonary changes with inhaled humid atmospheres: clinical application, Anesthesiology 30 (2) (1969) 199–207.
[22] R. Williams, N. Rankin, T. Smith, D. Galler, P. Seakins, Relationship between the humidity and temperature of inspired gas and the function of the airway mucosa, Crit. Care Med. 24 (11) (1996) 1920–1929.
[23] Y.Y. Zuo, A.W. Neumann, Pulmonary surfactant and its in vitro assessment using axisymmetric drop shape analysis (adsa): a review, Tenside, Surfactants, Detergents 42 (3) (2005) 126–147.
[24] J.J. Pillow, High-frequency oscillatory ventilation: Mechanisms of gas exchange and lung mechanics, Crit. Care Med. 33 (2005) (3 SUPPL.).
[25] L.M.Y. Yu, J.J. Lu, Y.W. Chan, A. Ng, L. Zhang, M. Hoorfar, Z. Policova, K. Grundke, A.W. Neumann, Constrained sessile drop as a new configuration to measure low surface tension in lung surfactant systems, J. Appl. Physiol. 97 (2) (2004) 704–715.
[26] S.M.I. Saad, Z. Policova, E.J. Acosta, A.W. Neumann, Axisymmetric drop shape analysis — constrained sessile drop (ADSA-CSD): a film balance technique for high collapse pressures, Langmuir 24 (19) (2008) 10843–10850.
[27] S.M.I. Saad, Z. Policova, A. Dang, E.J. Acosta, M.L. Hair, A.W. Neumann, A double injection ADSA–CSD methodology for lung surfactant inhibition and reversal studies, Colloids Surf. B: Biointerfaces 73 (2) (2009) 365–375.
[28] J.A. Clements, E.S. Brown, R.P. Johnson, Pulmonary surface tension and the mucus lining of the lungs: some theoretical considerations, J. Appl. Physiol. 12 (1958) 262–268.
[29] J.A. Clements, R.F. Hustead, R.P. Johnson, I. Gribetz, Pulmonary surface tension and alveolar stability, J. Appl. Physiol. 16 (3) (1961) 444–450.
[30] R.M. Prokop, A.W. Neumann, Measurement of the interfacial properties of lung surfactant, Curr. Opin. Colloid Interface Sci. 1 (1996) 677–681.
[31] S. Schürch, H. Bachofen, J. Goerke, F. Possmayer, A captive bubble method reproduces the in situ behavior of lung surfactant monolayers, J. Appl. Physiol. 67 (6) (1989) 2389–2396.
[32] S. Schürch, M. Lee, P. Gehr, Pulmonary surfactant: surface properties and function of alveolar and airway surfactant, Pure Appl. Chem. 64 (1992) 1747–1750.
[33] S. Schürch, H. Bachofen, Surfactant therapy for lung disease, Ch., Biophysical Aspects in the Design of a Therapeutic Surfactant, Marcel Dekker, New York, 1995, pp. 3–32.
[34] Y.Y. Zuo, R. Gitiafroz, E.J. Acosta, Z. Policova, P.N. Cox, M.L. Hair, A.W. Neumann, Effect of humidity on the adsorption kinetics of lung surfactant at air–water interfaces, Langmuir 21 (23) (2005) 10593–10601.
[35] R. Wüstneck, J. Perez-Gil, N. Wüstneck, A. Cruz, V.B. Fainerman, U. Pison, Interfacial properties of pulmonary surfactant layers, Adv. Colloid Interface Sci. 117 (1–3) (2005) 33–58.
[36] S.M.I. Saad, A.W. Neumann, E.J. Acosta, A dynamic compression-relaxation model for lung surfactants, Colloids Surf., A Physicochem. Eng. Asp. 354 (1–3) (2010) 34–44.
[37] E.C. Smith, J.M. Crane, T.G. Laderas, S.B. Hall, Metastability of a supercompressed fluid monolayer, Biophys. J. 85 (5) (2003) 3048–3057.
[38] Y.Y. Zuo, H. Alolabi, A. Shafiei, N. Kang, Z. Policova, P.N. Cox, E.J. Acosta, M.L. Hair, A.W. Neumann, Chitosan enhances the in vitro surface activity of dilute lung surfactant preparations and resists albumin-induced inactivation, Pediatr. Res. 60 (2) (2006) 125–130.
[39] Y. Rotenberg, L. Boruvka, A.W. Neumann, Determination of surface tension and contact angle from the shapes of axisymmetric fluid interfaces, J. Colloid Interface Sci. 93 (1) (1983) 169–183.
[40] P. Cheng, D. Li, L. Boruvka, Y. Rotenberg, A.W. Neumann, Automation of axisymmetric drop shape analysis for measurements of interfacial tensions and contact angles, Colloids Surf. 43 (2–3) (1990) 151–167.
[41] O.I. del Río, A.W. Neumann, Axisymmetric drop shape analysis: computational methods for the measurement of interfacial properties from the shape and dimensions of pendant and sessile drops, J. Colloid Interface Sci. 196 (2) (1997) 136–147.
[42] G. Loglio, U. Tesei, N.D. Innocenti, R. Miller, R. Cini, Non-equilibrium surface thermodynamics. measurement of transient dynamic surface tension for fluid–fluid interfaces by the trapezoidal pulse technique, Colloids Surf. 57 (2) (1991) 335–342.
[43] N. Wüstneck, R. Wüstneck, V.B. Fainerman, U. Pison, R. Miller, Investigation of over-compressed spread l-dipalmitoyl phosphatidylcholine films and the influence of solvent vapour in the gas phase on γ/a isotherms measured by using the captive bubble technique, Colloids Surf., A Physicochem. Eng. Asp. 164 (2–3) (2000) 267–278.
[44] L.F. Shampine, M.W. Reichelt, The Matlab Ode Suite, SIAM J. Sci. Comput. 18 (1) (1997) 1–22.
[45] J.C. Lagarias, J.A. Reeds, M.H. Wright, P.E. Wright, Convergence properties of the Nelder–Mead simplex method in low dimensions, SIAM J. Optim. 9 (1) (1999) 112–147.
[46] A. Pettenazzo, A.H. Jobe, M. Ikegami, E. Rider, S.R. Seidner, T. Yamada, Cumulative effects of repeated surfactant treatments in the rabbit, Exp. Lung Res 16 (2) (1990) 131–143.
[47] D. Hafner, P.G. Germann, D. Hauschke, Effects of lung surfactant factor (LSF) treatment on gas exchange and histopathological changes in an animal model of adult respiratory distress syndrome (ARDS): Comparison of recombinant LSF with bovine LSF, Pulm. Pharmacol. 7 (5) (1994) 319–332.
[48] D. Hafner, R. Beume, U. Kilian, G. Krasznai, B. Lachmann, Dose–response comparisons of five lung surfactant factor (LSF) preparations in an animal model of adult respiratory distress syndrome (ARDS), Br. J. Pharmacol. 115 (3) (1995) 451–458.
[49] J.F. Lewis, B. Tabor, M. Ikegami, A.H. Jobe, M. Joseph, D. Absolom, Lung function and surfactant distribution in saline-lavaged sheep given instilled vs. nebulized surfactant, J. Appl. Physiol. 74 (3) (1993) 1256–1264.
[50] J.F. Lewis, In vivo studies of aerosolized exogenous surfactant, Aerosol Sci. Technol. 22 (4) (1995) 354–363.
[51] J.F. Lewis, L.A. McCaig, D. Häfner, R.G. Spragg, R. Veldhuizen, C. Kerr, Dosing and delivery of a recombinant surfactant in lung-injured adult sheep, Am. J. Respir. Crit Care Med. 159 (3) (1999) 741–747.
[52] J.C. Meister, V. Balaraman, T. Ku, A. DeSilva, S. Sood, C.F.T. Uyehara, D.A. Person, D. Easa, Lavage administration of dilute recombinant surfactant in acute lung injury in piglets, Pediatr. Res. 47 (2) (2000) 240–245.
[53] S.B. Hall, M.S. Bermel, Y.T. Ko, H.J. Palmer, G. Enhorning, R.H. Notter, Approximations in the measurement of surface tension on the oscillating bubble surfactometer, J. Appl. Physiol. 75 (1) (1993) 468–477.
[54] C.H. Chang, E.I. Franses, An analysis of the factors affecting dynamic tension measurements with the pulsating bubble surfactometer, J. Colloid Interface Sci. 164 (1) (1994) 107–113.
[55] Y.C. Liao, O.A. Basaran, E.I. Franses, Effects of dynamic surface tension and fluid flow on the oscillations of a supported bubble, Colloids Surf., A Physicochem. Eng. Asp. 282–283 (2006) 183–202.

[56] A.L. Caro, M.R.R. Nio, J.M.R. Patino, The effect of ph on surface dilatational and shear properties of phospholipid monolayers, Colloids Surf. A: Physicochem. Eng. Aspects 327 (1–3) (2008) 79–89.
[57] G. Loglio, R. Miller, A. Stortini, U. Tesei, N.D. Innocenti, R. Cini, Nonequilibrium properties of fluid interfaces: aperiodic diffusion-controlled regime 2. experiments, Colloids Surf., A Physicochem. Eng. Asp. 95 (1) (1995) 63–68.
[58] R. Wüstneck, N. Wüstneck, B. Moser, V. Karageorgieva, U. Pison, Surface dilatational behavior of pulmonary surfactant components spread on the surface of a pendant drop. 1 - dipalmitoyl phosphatidylcholine and surfactant protein c, Langmuir 18 (4) (2002) 1119–1124.
[59] R. Wüstneck, N. Wüstneck, B. Moser, U. Pison, Surface dilatational behavior of pulmonary surfactant components spread on the surface of a pendant drop. 2 - dipalmitoyl phosphatidylcholine and surfactant protein b, Langmuir 18 (4) (2002) 1125–1130.
[60] N. Wüstneck, R. Wüstneck, U. Pison, Surface dilatational behavior of pulmonary surfactant components spread on the surface of a captive bubble. 3. dipalmitoyl phosphatidylcholine, surfactant protein c, and surfactant protein b, Langmuir 19 (18) (2003) 7521–7527.
[61] J. Perez-Gil, K.M.W. Keough, Interfacial properties of surfactant proteins, Biochim. Biophys. Acta - Mol. Basis Dis. 1408 (2–3) (1998) 203–217.